·基础研究·

ATM 失活诱导 GADD45α 依赖的小脑颗粒神经元凋亡

吴森斌[1]，伍健伟[2]，马　莹[1]，赵凡一[1]，曹东芳[1]，梁建峰[2]，胡坤华[3]，袁忠民[1]
（1. 广州医科大学附属第二医院神经科学研究所，广东 广州 510260；2. 广州医科大学附属第二医院番禺院区神经外科，广东 广州 511400；3. 中山大学中山医学院蛋白质组学实验室，广东 广州 510080）

摘　要：【目的】探究共济失调毛细血管扩张突变（ATM）激酶失活诱导神经元凋亡的具体分子机制。【方法】体外成熟 7 d 的小脑颗粒神经元（CGNs）分别用含 25 mmol/L KCl（25 K）培养基、5 mmol/L KCl（5 K）培养基和含 ATM 特异性抑制剂（Ku55933，10 μmol/L；Ku60019，15 μmol/L）的 25 K 培养基后进行免疫印迹检测 ATM、Caspase3、Cleaved Caspase-3 的蛋白表达水平或培养 8 h 后进行 Hoechst 染色分析。在 C6 细胞和 CGNs 中转染 ATM 和 GADD45α 特异性 siRNA，q-PCR 和免疫印迹验证其干扰效率。体外成熟 5 d 的 CGNs 通过磷酸钙转染 ATM 特异性 siRNA 和 pCMV-EGFP 48 h 后进行 Hoechst 染色和凋亡分析。体外成熟 7 d 的 CGNs 用含 ATM 特异性抑制剂的 25 K 培养基培养 8 h 后进行全转录组测序、差异表达基因鉴定和通路富集分析。体外成熟 5 d 的 CGNs 通过磷酸钙转染 GADD45α 特异性 siRNA 和 pCMV-EGFP 48 h，用含 15 μmol/L Ku6 的 25 K 培养基处理 8 h 或 5 K 培养基处理 8 h 后进行 Hoechst 染色和凋亡分析。【结果】与 25 K 组相比，5 K 处理组和 ATM 特异性抑制剂处理组的 CGNs ATM 蛋白表达降低、Cleaved Caspase-3 蛋白表达增加、细胞核固缩率增加。C6 细胞和 CGNs 中转染 ATM 和 GADD45α 特异性 siRNA 后有效降低 ATM 和 GADD45α 的 mRNA 和蛋白的表达。与对照相比，CGNs 转染 ATM 特异性 siRNA 后，细胞核固缩率升高。在 Ku55933 处理组中鉴定出 835 个基因表达上调，848 个基因表达下调；在 Ku60019 处理组中鉴定出 454 个基因表达上调，314 个基因表达下调；274 个基因在 Ku5 处理组和 Ku6 处理组中共同上调，179 个基因在 Ku5 处理组和 Ku6 处理组中共同下调，其中 ATM 下游靶标 GADD45α 表达上调；通路富集结果显示 TNF 信号通路、NF-κB 信号通路和凋亡信号通路等被显著富集。与对照相比，抑制剂处理组和 5K 组 GADD45α 的 mRNA 和蛋白表达均升高。与对照相比，转染 GADD45α 特异性 siRNA 后用含 15 μmol/L Ku60019 的 25 K 培养基处理 8 h 或 5 K 培养基处理后的 CGNs 细胞核固缩率降低。【结论】ATM 活性降低诱导 GADD45α 依赖的神经元凋亡。

关键词：神经元凋亡；共济失调毛细血管扩张突发；生长停滞和 DNA 损伤诱导蛋白 45α；转录组测序
中图分类号：R74　　**文献标志码：**A　　**文章编号：**1672-3554（2023）05-0758-10
DOI：10.13471/j.cnki.j.sun.yat-sen.univ（med.sci）.2023.0506

Loss of ATM activity induces GADD45α-dependent apoptosis in cerebellar granular neurons

WU Sen-bin[1], WU Jian-wei[2], MA Ying[1], ZHAO Fan-yi[1], CAO Dong-fang[1], LIANG Jian-feng[2], HU Kun-hua[3], YUAN Zhong-min[1]
（1. Institute of Neuroscience, The Second Affiliated Hospital of Guangzhou Medical University, Guangzhou 510260, China; 2. Neurosurgery Department, The Second Affiliated Hospital of Guangzhou Medical University, Panyu District, Guangzhou 511400, China; 3. Proteomics Center, Zhongshan School of Medicine, Sun Yat-sen University, Guangzhou 510080, China）
Correspondence to: YUAN Zhong-min; E-mail: yzm@gzhmu.edu.cn

Abstract:【objective】To explore the specific molecular mechanism of neuronal apoptosis induced by ATM inactivation.【Methods】CGNs matured 7 days in vitro were cultured 8 h with 25 K, 5 K or 25 K medium containing ATM-specific

收稿日期：2023-05-31
基金项目：国家科技部纵向子课题（2016YEC1301703）；广东省自然科学基金（2019A1515010473；2021A1515010780）；广东省联合培养研究生示范基地项目（2023）；广州市科学技术局基金（202002020088）
作者简介：吴森斌，第一作者；袁忠民，通信作者，研究员，E-mail：yzm@gzhmu.edu.cn

inhibitors (Ku55933, 10 μmol/L; Ku60019, 15 μmol/L) for Hoechst stain and apoptosis analysis, or cultured for different lengths of time (2, 4, 8 h) to detect the protein expression levels of ATM, caspase-3 and cleaved caspase-3 by Western blotting. ATM and GADD45α specific siRNA was transfected into C6 cells and CGNs, and its interference efficiency was verified by q-PCR and Western blotting. CGNs matured for 5 days in vitro were transfected with ATM specific siRNA and pCMV-EGFP by calcium phosphate for 48 h, Hoechst staining and apoptosis analysis were performed. CGNs matured for 7 days in vitro were treated with 25 K medium containing ATM specific inhibitors for 8 h, transcriptome sequencing, differential expression gene identification and pathway enrichment analysis were performed. CGNs matured for 5 days in vitro were co-transfected with GADD45α specific siRNA and pCMV-EGFP by calcium phosphate for 48 h, then treated with 5 K or 25 K medium containing 15 μmol/L Ku6 for 8 h. Hoechst staining and apoptosis analysis were performed.【Results】Compared with the 25 K, CGNs nuclear pyknosis rate, cleaved Caspase-3 and ATM protein expression level were increased in the 5 K and ATM-specific inhibitor groups. The mRNA and protein expression levels of ATM and GADD45α were effectively reduced after transfection of ATM and GADD45α specific siRNA in C6 cells and CGNs. Compared with control, CGNs transfected with ATM specific siRNA showed a higher nuclear pyknosis rate. Totally 835 genes were identified to be up-regulated and 848 genes to be down-regulated in the Ku55933 treatment group; 454 genes were identified to be up-regulated and 314 genes to be down-regulated in the Ku6 treatment group; 274 genes were co-up regulated in the Ku5 and Ku60019 treatment groups, while 179 genes were co-down-regulated in the Ku5 and Ku6 treatment groups and the expression of ATM downstream target GADD45α was upregulated. The enrichment results showed that TNF signaling pathway, NF-κB signaling pathway and Apoptosis signaling pathway were significantly enriched. Compared with control, mRNA and protein expression levels of GADD45α were increased in inhibitor treatment and 5 K, while knocking down GADD45α resulted in a decrease in nuclear pyknosis rate in the Ku60019 and 5 K treatment group.【Conclusion】Loss of ATM activity induces GADD45α-dependent cerebellar granular neuronal apoptosis.

Key words: neuronal apoptosis; ATM; GADD45α; transcriptome sequencing

[J SUN Yat-sen Univ(Med Sci),2023,44(5):758-767]

共济失调毛细血管扩张突变(ataxia-telangiectasia mutated, ATM)激酶首发于一种由该基因突变导致的人类常染色体隐性遗传疾病共济失调-毛细血管扩张症中，该疾病主要特征是为小脑进行性变性和颗粒神经元的丢失表现为共济失调[1]。ATM激酶作为神经元内响应DNA损伤的关键调控蛋白和DNA损伤修复反应的关键组成部分，激活后会磷酸化多种底物靶蛋白以参与DNA双链断裂修复、细胞周期检查点阻滞和细胞凋亡等过程[2]。这些依赖于ATM的磷酸化事件对于阻止细胞周期进程、允许DNA修复或诱导细胞凋亡是必不可少的[3-4]。在神经元变性丢失过程中，DNA损伤被认为是神经元死亡的广泛引发因素，也是各种神经系统疾病的基本机制[2,5-6]。目前，尚不清楚ATM活性缺失是否通过诱导神经元凋亡导致小脑进行性变性和颗粒神经元的丢失。本研究利用ATM特异性抑制剂和siRNA处理大鼠小脑颗粒神经元，观察对小脑颗粒神经元凋亡的影响，通过全转录组测序以探讨ATM活性缺失诱导小脑颗粒神经元凋亡的机制。

1　材料与方法

1.1　实验材料

高糖培养基DMEM、0.25%胰酶、FBS、青霉素-链霉素P/S、L-glutamine和PBS均购自Gibco公司，Trypsin、DNase、阿糖胞苷、Poly-L-lysine、BME和D-(+)glucose均购自Sigma公司，KCl、Trypsin inhibitor、BSA、$CaCl_2$、$MgSO_4$•$7H_2O$均购自上海生工公司，RT-qPCR试剂购自日本Toyobo公司。96孔板和6孔板购自NEST公司，Anti-ATM购自CST和Abcam公司，Anti-GADD45α、Anti-Cleaved Caspase-3和Anti-Caspase3均购自CST公司，Anti-GAPDH购自Proteintech公司。HRP-conjugated Goat Anti-Mouse IgG和HRP-conjugated Goat Anti-Rabbit IgG购自上海生工公司，RNAiMax购自Thermo公司，ProFection® Mammalian Transfection System购自Promega公司。

1.2　实验方法

1.2.1　小脑颗粒神经元和C6细胞培养及药物处理方法　小脑颗粒神经元的制备和培养如前所述。

简单来说从7～8日龄Sprague-Dawley幼鼠(购自南方医科大学实验动物中心,伦理编号:A2021-009)中分离小脑,去除血管网后将其切割成0.65 cm×0.65 cm方块大小,用含胰蛋白酶的Crebs缓冲液消化15 min后终止消化,离心重悬成单细胞悬液,并用含有25 mmol/L KCl、10% FBS的和1% P/S的基础培养基BME接种。接种18 h后加入阿糖胞苷(终浓度10 μmol/L)。体外培养7 d成熟后,将神经元转换为含25 mmol/L KCl (25 K)的无血清BME培养基同时给予指定药物处理指定时间。Ku55933和Ku60019储存浓度分别为10 μmol/L×1 000和15 μmol/L×1 000使用时用培养基1 000倍稀释。大鼠胶质瘤细胞系C6细胞(购自中国科学院细胞库并采用短串联重复DNA指纹图谱进行鉴定)在含有10 g/L胎牛血清、100 U/mL青霉素和100 μg/mL链霉素的DMEM中培养,置于体积分数5% CO_2, 37 ℃细胞培养箱中培养[7]。

1.2.2 Western blotting检测ATM、Cleaved Caspase-3、Caspase3和GADD45α蛋白的表达 用含蛋白酶抑制剂的细胞裂解液裂解细胞收集后进行超声破碎,离后收集上清,并通过BCA蛋白定量试剂盒(Thermo,#23225)测定细胞样本蛋白浓度。根据检测目标蛋白质的分子量,选用适当浓度的聚丙烯酰胺凝胶进行电泳分离蛋白质裂解物,然后转移到PVDF膜中。用体积分数5%脱脂奶封闭1 h后,分别用一抗(Anti-GADD45α、Anti-Cleaved Caspase-3、Anti-Caspase3、Anti-GAPDH)4 ℃孵育过夜后用二抗(HRP标记抗兔或抗鼠二抗)室温孵育1 h并进行ECL显影。

1.2.3 ATM和GADD45α特异性siRNA转染和相关基因的mRNA表达 ATM和GADD45α特异性siRNA购自吉玛基因,目标基因siRNA和对照siRNA(siNC)根据制造商的标准方案通过RNAiMax转染到大鼠C6胶质瘤细胞以验证其干扰效率,转染48 h后收集细胞,用Trizol法提取分离细胞总RNA并进行逆转录,逆转录后进行RT-qPCR检测相关基因的mRNA表达水平。特异性siRNA序列见表1,引物序列见表2[8]。使用算式ratio=$2^{-\Delta\Delta Ct}$计算上述基因的相对表达。

1.2.4 磷酸钙法转染神经元及Hoechst染色 CGNs按3×10^6个/孔的数量接种到ploy-lysine包被过夜的六孔板中,在接种后第4~5天切换无血清的BME培养基,用ProFection® Mammalian Transfection System转染试剂按每孔pCMV-N-EGFP质粒2 μg:siRNA 6 μg加到150 μL的2×HEPEs中,并与150 μL的带有37 μL $CaCl_2$的2×HEPEs涡旋混匀后静置2~3 min后立即将混合物滴加入对应孔中37℃细胞培养箱中培养1 h,弃含有磷酸钙转染试剂的培养基后用MEM培养基洗两次加新鲜培养基转染48 h后给予相应的处理。为了评估目标基因特异性siRNA对细胞凋亡率的影响,我们使用EGFP标记共转染细胞。处理结束后,去除培养基并在室温下用40 g/L多聚甲醛固定30 min。去除40 g/L多聚甲醛后用PBS洗两遍后将细胞与10 μg/mL的Hoechst 33258在室温下孵育15 min,在荧光显微镜下观察其核染色。在荧光显微镜下表现出核固缩的细胞被认为是凋亡细胞。通过计算EGFP阳性神经元群中核固缩的百分比来测定细胞凋亡率[8]。

1.2.5 全转录组测序和分析 使用Trizol法提取并分离CGNs总RNA,对于测序样本,后续的样本质检、文库构建和Illumina测序均由诺禾致源(Novogene)公司完成。差异基因分析首先对原始的read-

表1 siRNA序列

Table 1 Special siRNA sequences of ATM and GADD45α

Name	Sequence
siGADD45α-1	5′ GGAUCCUGCCUUAAGUCAATT 3′
siGADD45α-2	5′ GGAAAGUCGCUACAUGGAUTT 3′
siATM-1	5′ GGUCUACGAUACUCUUAAATT 3′
siATM-1	5′ GGUCUACGAUACUCUUAAATT 3′

表2 RT-qPCR引物序列

Table 2 Primers of related genes

Name		Sequence
GADD45α	forward	5′ GCAGAAGATCGAAAGGATGG 3′
	reverse	5′ GTACACGCCGACAGTTATGG 3′
ATM	forward	5′ ACATGAGCGTGGAGGATTTC 3′
	reverse	5′ GCAATGGACTTCACCTCATCA 3′
β-actin	forward	5′ CAACTGGGACGATATGGAGAAG 3′[8]
	reverse	5′ TCTCCTTCTGCATCCTGTCAG 3′[8]

count进行标准化，主要是对测序深度的校正。使用DESeq2软件（1.20.0）进行两个比较组合之间的差异表达分析，然后通过统计学模型进行假设检验概率（*P*-value）的计算，最后进行多重假设检验校正后得到$P_{(adj)}$，其中以$P_{(adj)}$ < 0.05和|log2FoldChange| > 1作为差异表达基因的筛选阈值。测序后分析平台：诺禾云平台（magic.novogene.com）。京都基因和基因组百科全书（KEGG）富集分析被用于探索与候选差异表达基因相关的信号通路。

1.3　统计学方法

使用SPSS软件进行统计学分析并用GraphPad Prism进行可视化，计量资料采用均数±标准差（$\bar{x}\pm s$）表示。两组间比较采用两独立样本*t*检验。3组及以上样本的均数比较采用单因素方差分析，随后的组间比较如符合方差齐性采用LSD法，否则采用Dunnett-*t*3检验。*P*<0.05被认为差异具有统计学意义。

2　结果

2.1　ATM在5K诱导的CGNs凋亡中蛋白水平降低

将体外成熟7 d的CGNs从细胞外25 mmol/L KCl（25 K）条件切换到5 mmol/L KCl（5 K）条件作用8 h后进行hoechst染色，可观察到CGNs表现出典型的细胞凋亡特征，细胞核皱缩，染色体凝聚形成凋亡小体（图1A）。在25 K条件下细胞核固缩率为（17.60 ± 1.62）%，切换到5 K条件后细胞核固缩率增加到（61.87 ± 2.57）%，差异具有统计学意义（*t*=-32.586，*P*=0.000；图1B）。蛋白印迹检测了细胞凋亡的关键执行蛋白Caspase-3。结果显示，与25 K条件相比，5 K处理不同时间（2、4、8 h）后均检测到剪切激活的Cleaved Caspase-3；此外5 K处理不同时间后也检测到ATM蛋白表达水平降低，差异具有统计学意义（ATM：*F*=182.341，*P*=0.000；Cleaved Caspase-3：*F*=393.504，*P*=0.000；图1C，D）。

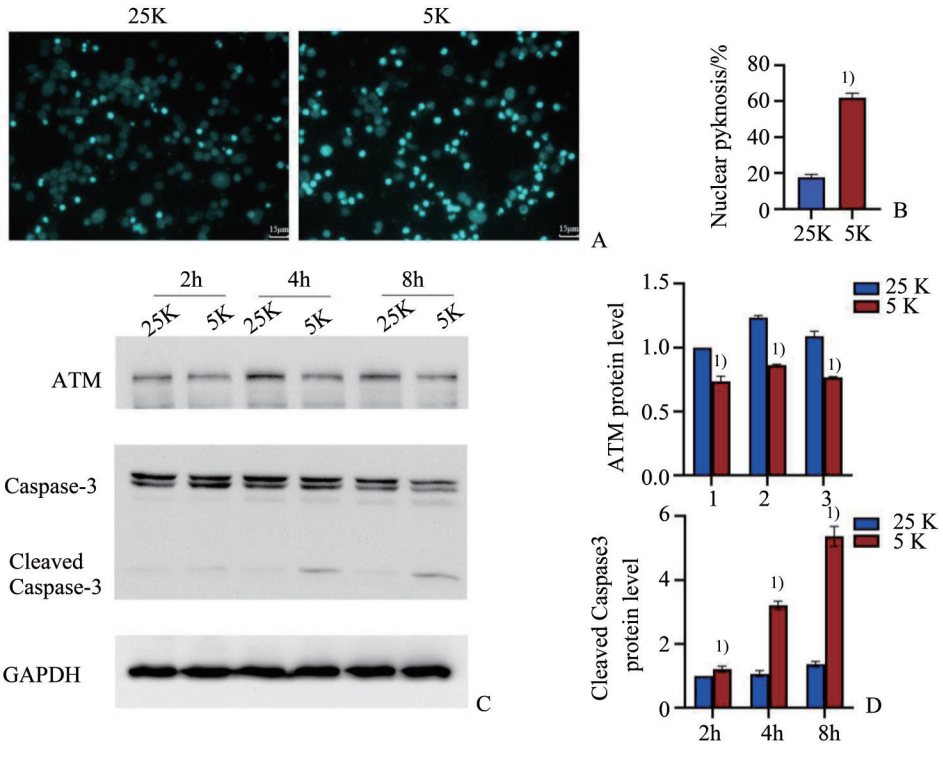

A: CGNs matured for 7 days in vitro were cultured with 25 K and 5 K medium for 8 h and analyzed by Hoechst staining. Representative fluorogram of nuclear staining (scale, 15 μm). B: 1) *P* < 0.05, compared with 25 K group. C: CGNs matured for 7 days in vitro were cultured in 25 K and 5 K medium for different time, respectively, and the protein expression levels of ATM, Caspase-3 and Cleaved Caspase-3 were detected by western blot. D: The relative density of ATM and Cleaved Caspase-3 were analyzed by Image J software. 1) *P* < 0.05, compared with 25 K group. *n*=3.

图1　在5 K诱导的CGNs凋亡中ATM蛋白表达降低

Fig. 1　ATM protein expression was decreased in CGNs apoptosis induced by 5 K

2.2 药理学或siRNA抑制ATM后诱导CGNs发生细胞凋亡

2.2.1 药理学抑制ATM活性诱导CGNs发生典型的细胞凋亡 为了探讨抑制ATM活性后是否诱导CGNs发生典型的细胞凋亡,在25 K条件下,用10 μmol/L Ku55933和15 μmol/L Ku60019以抑制ATM活性。Hoechst染色结果显示与对照相比,ATM特异性抑制剂作用8 h后均观察到CGNs典型的细胞凋亡特征,核固缩率显著升高,差异具有统计学意义(F=246.311, P=0.000;图2 A, B)。免疫印迹结果显示,与25 K组相比,ATM特异性抑制剂作用不同时间均检测到ATM蛋白表达降低,同时也检测到切割活化的Cleaved Caspase-3,差异具有统计学意义(ATM: F=64.422, P=0.000; Cleaved Caspase-3: F=300.142, P=0.000;图2 C, D)。

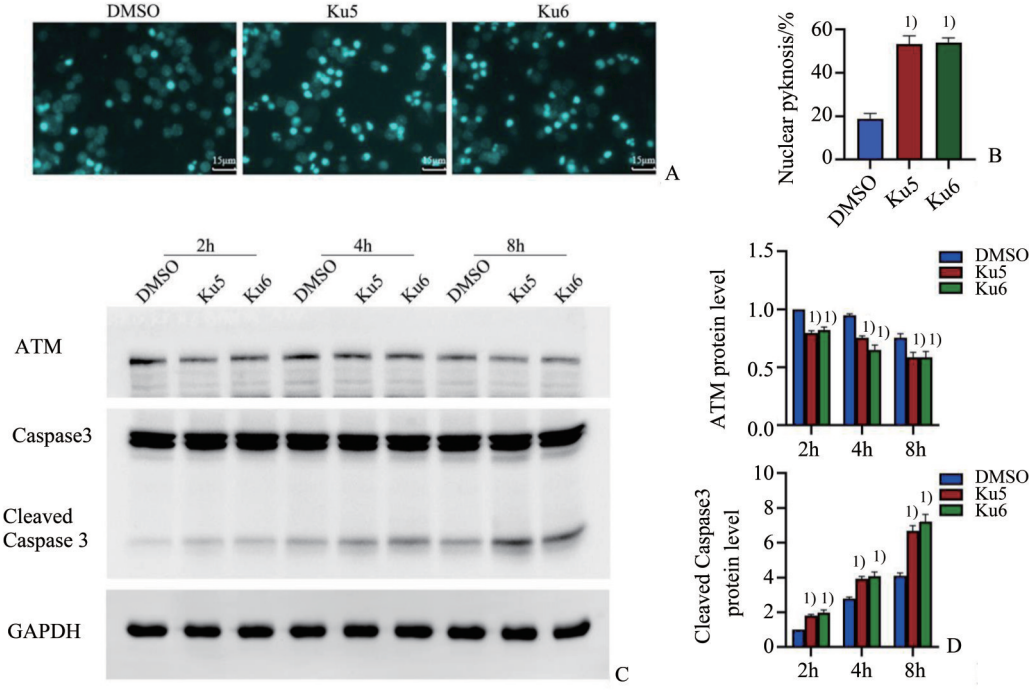

A: CGNs matured for 7 days in vitro were cultured in 25 K medium with or without ATM-specific inhibitors for 8 h and analyzed by Hoechst staining. Representative fluorogram of nuclear staining (scale, 15 μm). B: 1) P < 0.05, compared with DMSO group. C: CGNs matured for 7 days in vitro were cultured in 25 K medium with or without ATM-specific inhibitors for different time, respectively and the protein expression levels of ATM, Caspase-3 and Cleaved Caspase-3 were detected by Western blotting. D: The relative density of ATM and Cleaved Caspase-3 were analyzed by ImageJ software. 1) P < 0.05, compared with DMSO group. Ku5: Ku55933, Ku6: Ku60019. n=3.

图2 药理学抑制ATM活性诱导CGNs发生典型的细胞凋亡

Fig. 2 Pharmacological inhibition of ATM activity induced apoptosis of CGNs cells

2.2.2 siRNA抑制ATM诱导CGNs发生典型的细胞凋亡 由于药理抑制剂可能具有非靶向作用,随后引入了siRNA以特异性地敲低ATM。首先在C6细胞中验证siRNA的干扰效率。在C6细胞中分别转染siATM-1和siATM-2两个干扰片段,并以siNC片段为阴性对照,结果显示,与对照相比,ATM特异性siRNA可以有效降低ATM的mRNA水平,差异具有统计学意义(F=1 279.378, P=0.000;图3A)。CGNs在体外培养5 d后在25 K条件下通过磷酸钙转染ATM特异性siRNA 48 h后进行免疫印迹,结果显示,与对照相比,ATM特异性siRNA可以有效地阻断CGNs中ATM表达,差异具有统计学意义(F=7 143.042, P=0.000;图3B, C);此外,共转染ATM特异性siRNA和EGFP质粒后hoechst染色结果显示,沉默ATM后也观察到CGNs典型的凋亡特征,核固缩率显著增加,差异具有统计学意义(F=8.053, P=0.020;图3D)。

2.3 抑制ATM后转录组测序分析及验证

2.3.1 抑制ATM后转录组测序分析 为了进一步阐明抑制ATM诱导CGNs凋亡的具体作用机制,药

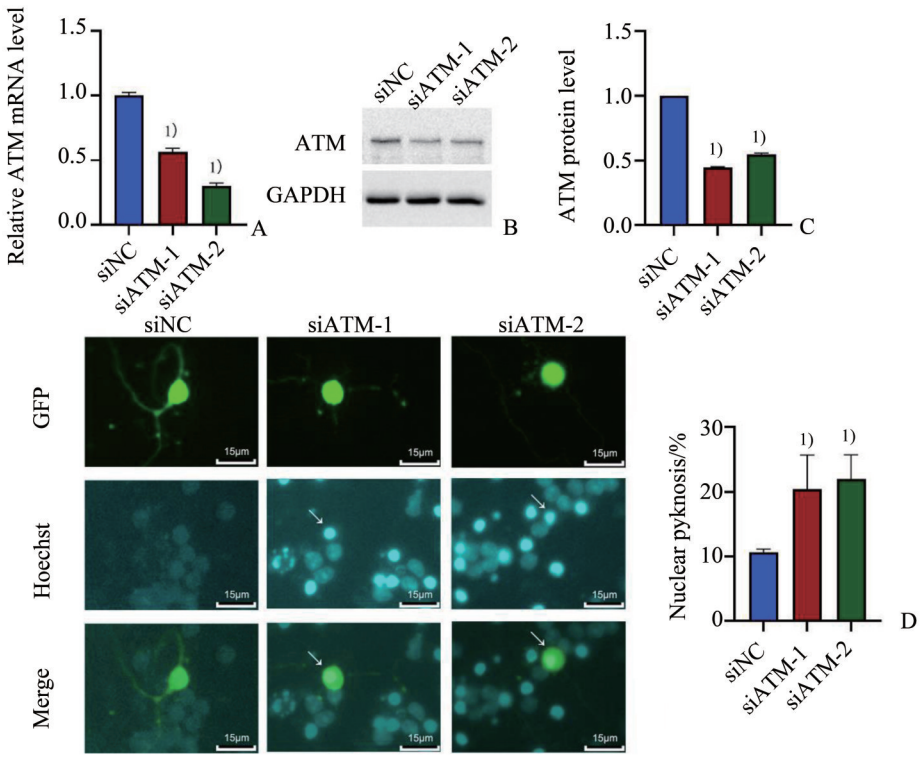

A: C6 cells transfected with ATM specific siRNA for 48 h and RT-qPCR was performed to detect ATM mRNA levels. 1) $P<0.05$, compared with siNC group. B: CGNs mature for 5 days in vitro were transfected with ATM specific siRNA by calcium phosphate for 48 h, and the ATM protein expression level was detected by Western blotting. C: The relative density of ATM was analyzed by ImageJ software. 1) $P<0.05$, compared with siNC group. D: Hoechst staining and apoptosis analysis were performed after transfection of CGNs with ATM specific siRNA and pCMV-EGFP 48 h. White arrows indicate transfected cells. bar=15 μm. 1) $P<0.05$, compared with siNC group. $n=3$.

图3　siRNA抑制ATM诱导CGNs发生典型的细胞凋亡

Fig. 3　SiRNA inhibits ATM induced typical cell apoptosis in CGNs

理学抑制ATM后，我们进行了全转录组测序。主成分分析（常用来评估组间差异及组内样本重复情况）结果显示Ku5处理组、Ku6处理组、5 K处理组和对照组的CGNs样本被很好地分离为不同的类群，且组内样本相似性较高（图4A）。差异表达基因热图显示，与25 K相比，药理学抑制ATM和5 K处理后基因表达模式显示出显著不同的（图4B）。通过转录组测序，我们共鉴定出835个基因在Ku5处理组中表达上调，848个基因表达下调；454个基因在Ku6处理组中表达上调，314个基因表达下调（图4C，D）。Veen图显示274个基因在Ku5处理组和Ku6处理组中共同上调，179个基因在Ku5处理组和Ku6处理组中共同下调（图4E，F）。在此基础上进行KEGG通路富集分析以探索具体机制。KEGG分析结果表明，TNF信号通路、NF-κB信号通路和凋亡信号通路等被显著富集（图4G）。ATM的下游靶标GADD45α在抑制ATM后显著上调。

2.3.2　*差异表达基因验证*　为了进一步验证GADD45α在抑制ATM活性后诱导CGNs凋亡中的表达水平，我们通过RT-qPCR和免疫印迹分别检测了其mRNA和蛋白表达。RT-qPCR结果显示，与转录组测序结果一致，ATM活性降低后GADD45α的mRNA水平显著升高，差异具有统计学意义（药理学抑制ATM：$F=1253.479$，$P=0.000$；5 K处理：$F=124.138$，$P=0.000$ 图5A，B）。免疫印迹结果也显示，GADD45α蛋白水平在药理学抑制ATM活性或在5 K处理不同时间（2、4、8 h）后均显著上调，差异具有统计学意义（药理学抑制ATM：$F=127.239$，$P=0.000$；5 K处理：$F=107.681$，$P=0.000$；图5C-E）。

2.4　GADD45α介导ATM活性降低引起的CGNs凋亡

为了进一步确定抑制ATM是否是通过上调GADD45α的表达诱导CGNs发生细胞凋亡，引入

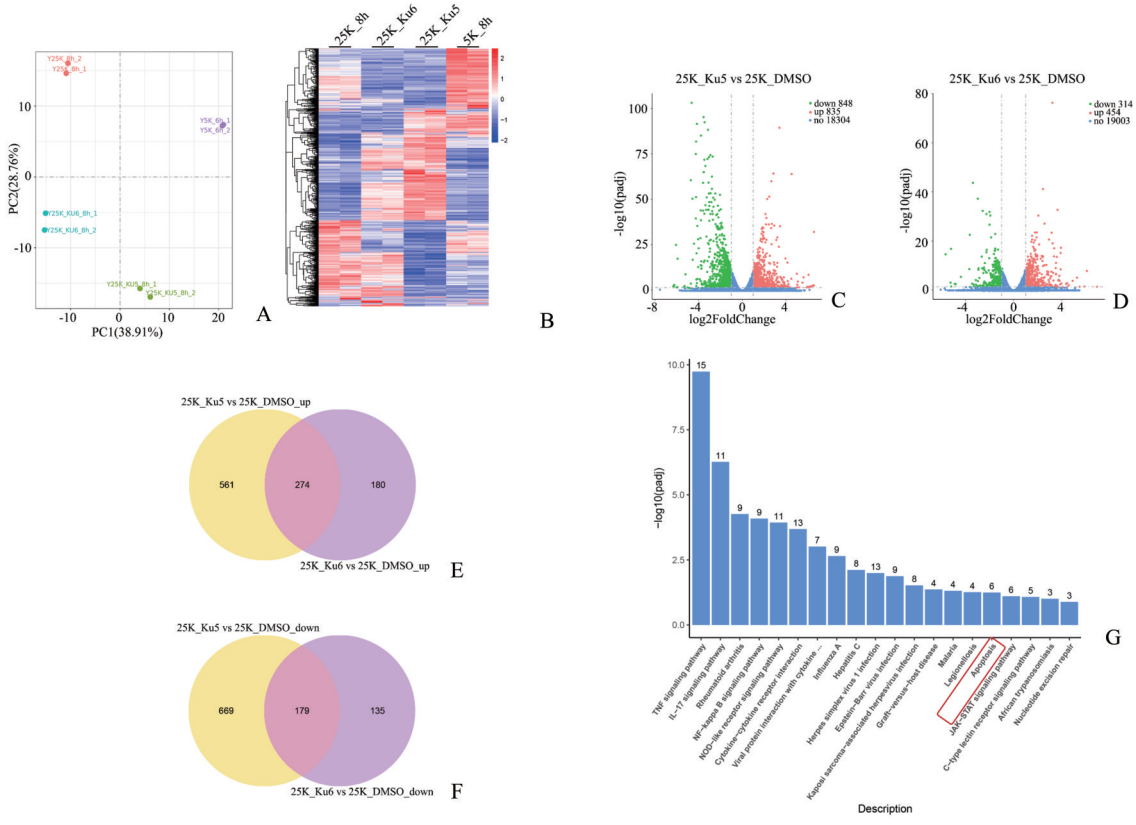

CGNs matured for 7 days in vitro were cultured in 25 K medium with or without ATM-specific inhibitors for 8 h and transcriptome sequencing was performed. A: principal component analysis (PCA). B: Heat map of differential gene expression. Ordinate represents gene clustering; The abscissa represents the clustering of samples. Red means upward, blue means downward. C, D: Volcano map of differentially expressed genes. Green dot: down-regulated differential gene; Red dots: up-regulated differential genes; Blue dots, no differentially expressed genes. E, F: Veen map of differentially expressed genes. G: KEGG pathway enrichment analysis of differentially expressed genes.

图4 药理学抑制ATM后转录组测序分析

Fig. 4 Transcriptome sequencing after pharmacologic inhibition of ATM

siRNA以特异性沉默GADD45α。首先在大鼠C6胶质瘤细胞中,siRNA可以降低内源性GADD45α的mRNA表达,差异具有统计学意义(F=56.105, P=0.000;图6A)。在CGNs中siGADD45α片段有效地降低GADD45α的蛋白水平,差异具有统计学意义(F=1707.429, P=0.000;图6B, C)。CGNs共转染siGADD45α片段和pCMV-PEGFP质粒48 h后用Ku6处理8 h或5 K条件处理8 h后均观察到CGNs细胞凋亡显著减少,差异具有统计学意义(5 K处理: F=476.213, P=0.000, Ku6: F=31.509, P=0.000;图6D, E)。

3 讨 论

细胞凋亡是机体内一种被严格调控的程序性细胞死亡模式。凋亡细胞的主要细胞形态学特征包括核收缩、染色体凝聚和DNA碎片化[9]。神经元细胞凋亡在发育和病理过程中广泛发生,由于成熟的神经元增殖或被替换的能力有限,因此神经元细胞凋亡这一过程尤其重要[10]。不适当的神经元凋亡与各种神经系统疾病中的大量神经元变性丢失有关,如阿尔茨海默病、亨廷顿舞蹈症和肌萎缩性侧索硬化症等[11-13]。

在神经元细胞死亡过程中,DNA损伤被认为是神经元凋亡的广泛引发因素,而ATM激酶是细胞内响应DNA损伤的关键调控蛋白[14-15]。近年来,ATM已经被广泛研究以阐明其在DNA损伤应答和共济失调毛细血管扩张症中发病机制中的作用[16]。尽管目前已经有数百种蛋白被鉴定为ATM磷酸化靶点,ATM的重要功能也逐步被阐明,然而,导致

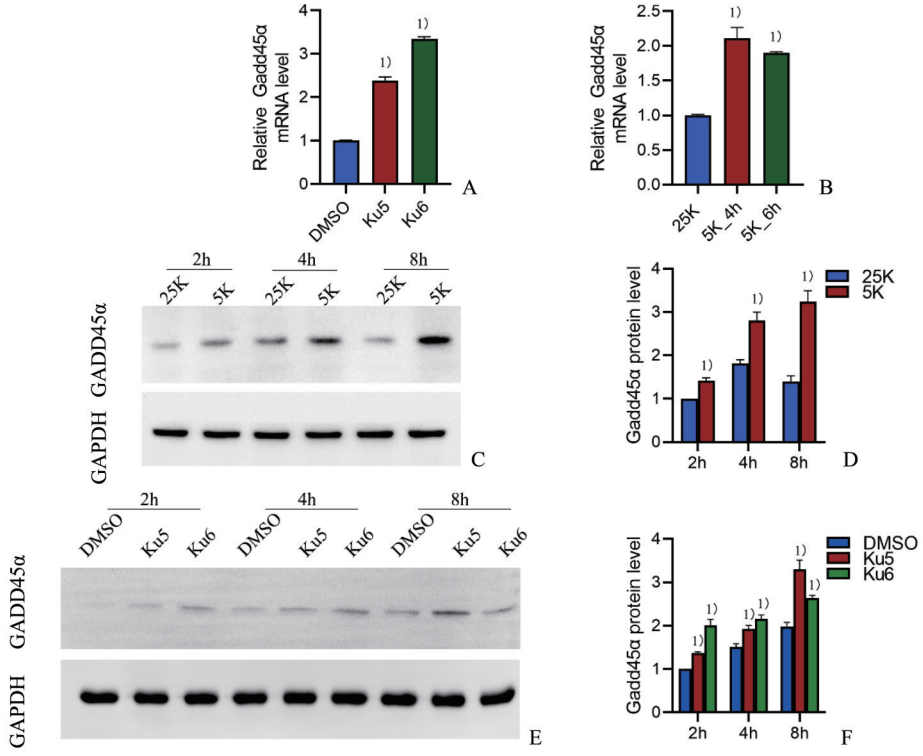

A: CGNs matured for 7 days in vitro were treated with or without ATM specific inhibitors for 8 h and RT-qPCR was performed to verify the mRNA expression level of GADD45α. 1) $P<0.05$, compared with DMSO group. B: CGNs matured for 7 days in vitro were cultured with 25 K and 5 K medium for 8 h and RT-qPCR was performed to detect the mRNA expression level of GADD45α. 1) $P<0.05$, compared with 25 K group. C: CGNs matured for 7 days in vitro were cultured with 25 K and 5 K medium for 8 h and western blotting was performed to detect the expression level of GADD45α protein. D: The relative density of GADD45α was analyzed by ImageJ software. 1) $P<0.05$, compared with 25 K group. E: CGNs matured for 7 days in vitro were treated with or without ATM specific inhibitors for 8 h and western blotting was performed to verify the protein expression level of GADD45α. F: The relative density of GADD45α was analyzed by ImageJ software. 1) $P<0.05$, compared with DMSO group. $n=3$.

图5　差异表达基因验证

Fig. 5　Validation of differentially expressed gene

神经系统中ATM依赖性细胞死亡的分子事件尚不清楚。因此探索ATM控制细胞凋亡的具体分子机制对理解神经系统疾病中神经元丢失过程和筛选相关治疗药物有积极作用。我们的研究发现在药理学抑制ATM活性或特异性siRNA沉默ATM后均能导致小脑颗粒神经元发生细胞凋亡，并能观察到典型的核固缩，其活性的缺失可能导致DNA修复的抑制和胞内DNA的积累最终导致基因毒性应激，神经细胞死亡。我们通过转录组测序和分析发现在抑制ATM或5K条件诱导小脑颗粒神经元发生细胞凋亡后均检测到GADD45α的mRNA和蛋白表达水平上调。GADD45α作为一种生长阻滞和DNA损伤诱导蛋白在各种细胞功能中起着至关重要的调节作用，例如DNA修复，细胞周期调节和衰老以及遗传毒性应激反应等[17]。据报道，GADD45a激活或过表达可抑制细胞生长并诱导细胞死亡。GADD45a在体外和体内的过表达显着损害了发育过程中神经元的形态，降低了新皮层神经元的神经突触的复杂性，诱导体细胞肥大并增加细胞死亡[18]。我们的研究也显示用特异性siRNA敲降GADD45α后再抑制ATM活性或5 K条件诱导小脑颗粒神经元发生凋亡减少。有研究表明在基因毒性应激情况下，p53，p38，Brca1等多种蛋白可以调控GADD45家族的转录[19-20]，其中转录因子Brca1可结合在GADD45α的启动子上以促进GADD45α的转录。我们RT-qPCR结果也显示Brca1的mRNA水平在抑制ATM后显著上升(结果未展示)。此外，有研究报道GADD45α蛋白的诱导表达导致Bim从微管相关成分解离并易位到线粒体。Bim在线粒体中的积累增强了Bim与Bcl-2的相互作用，从Bcl-2复合物

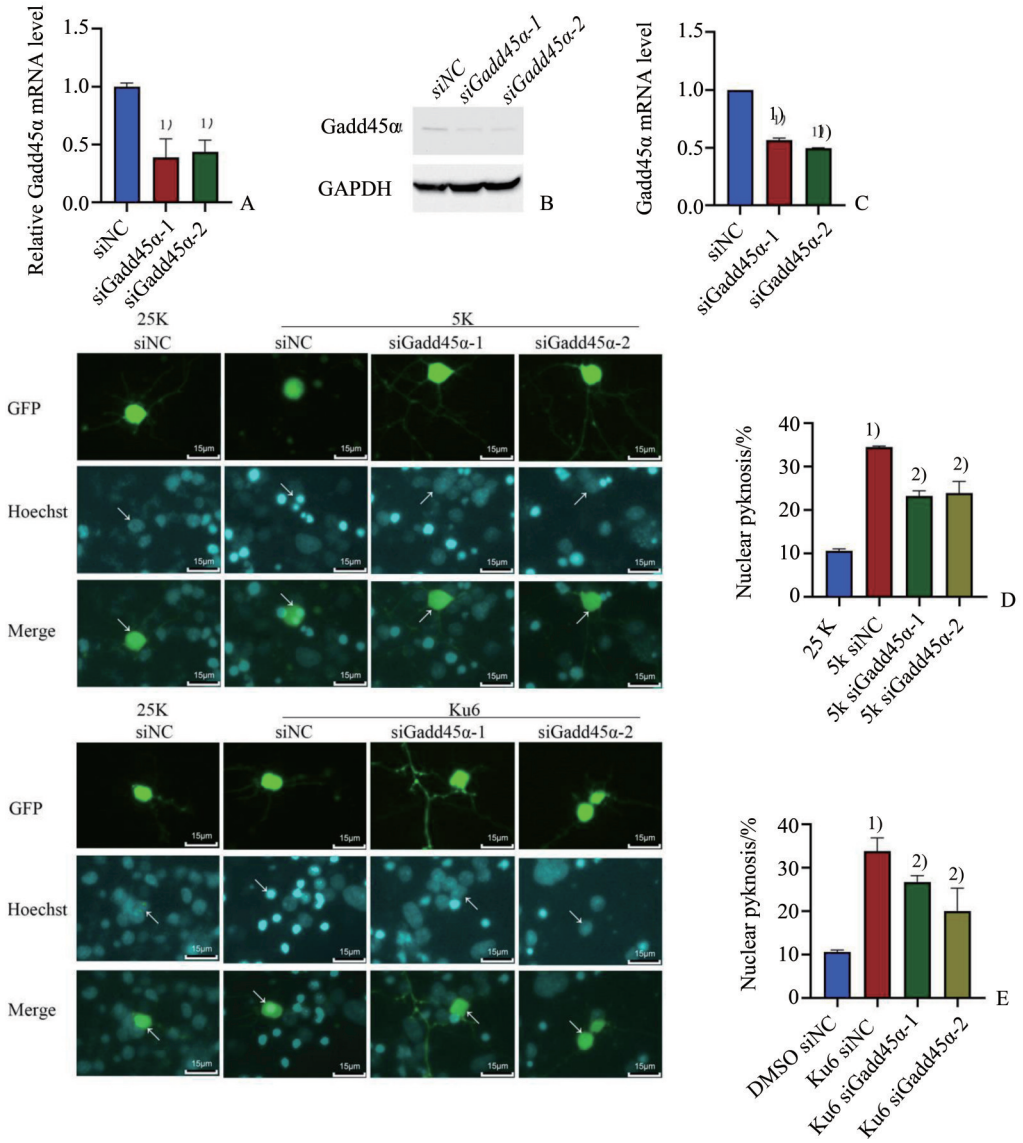

A: C6 cells were transfected with GADD45α specific siRNA for 48 h and RT-qPCR was performed to detect mRNA levels of GADD45α. 1) $P<0.05$, compared with siNC group. B: CGNs mature for 5 days in vitro were transfected with GADD45α specific siRNA by calcium phosphate for 48 h, and the GADD45α protein expression level was detected by western blotting. C: The relative density of GADD45αwas analyzed by ImageJ software. 1) $P<0.05$, compared with siNC group. D: CGNs was co-transfected with GADD45α siRNA and pCMV-EGFP plasmid for 48 h, treated with Ku6 for 8 h, and Hoechst staining and apoptosis analysis were performed. The white arrows represent transfected cells. 1) $P<0.05$, compared with 25 K siNC group. 2) $P<0.05$, compared with 5K siNC group. E: CGNs was co-transfected with GADD45α siRNA and pCMV-EGFP plasmid for 48 h, treated with 5K for 8 h, and Hoechst staining and apoptosis analysis were performed. The white arrows represent transfected cells. 1) $P<0.05$, compared with 25K siNC group. 2) $P<0.05$, compared with Ku6 siNC group. $n=3$. bar=15 μm .

图6 siRNA敲低GADD45α减少ATM活性降低引起的CGNs凋亡

Fig. 6 siRNA knockdown of GADD45α reduces CGNs apoptosis caused by decreased ATM activity

中释放Bax,导致细胞色素c释放到细胞质中最终诱导细胞凋亡[21-24]。ATM活性缺失通过何种机制上调GADD45α表达,尚需进一步研究。

总之,本研究显示ATM活性缺失导致GADD45α的表达增加,激活Caspase3,进而诱导小脑颗粒神经元发生凋亡。

参考文献

[1] Rothblum-oviatt C, Wright J, Lefton-greif MA, et al. Ataxia telangiectasia: a review[J]. Orphanet J Rare Dis, 2016, 11(1): 159.

[2] Putti S, Giovinazzo A, Merolle M, et al. ATM kinase dead: from ataxia telangiectasia syndrome to cancer[J]. Cancers (Basel), 2021, 13(21):5498.

[3] Blackford AN, Jackson SP. ATM, ATR, and DNA-PK: the trinity at the heart of the DNA damage response[J]. Mol Cell, 2017, 66(6): 801-817.

[4] Levi H, Bar E, Cohen-adiv S, et al. Dysfunction of cerebellar microglia in ataxia-telangiectasia[J]. Glia, 2022, 70(3): 536-557.

[5] Chan SF, Sances S, Brill LM, et al. ATM-dependent phosphorylation of MEF2D promotes neuronal survival after DNA damage[J]. J Neurosci, 2014, 34(13): 4640-4653.

[6] Fu X, Wan S, Lyu YL, et al. Etoposide induces ATM-dependent mitochondrial biogenesis through AMPK activation[J]. PLoS One, 2008, 3(4): e2009.

[7] 曹娅莉，吴力强，刘锶锶，等. 抑制HDAC4减少JNK/c-Jun活性及其依赖的神经元凋亡[J]. 中山大学学报(医学版)，2018，39(5)：669-674.
Cao YL, Wu LQ, Liu SS, et al. Inhibiting HDAC4 reduces JNK/c-Jun activity-dependent neuronal apoptosis[J]. J Sun Yat-Sen Univ (Med Sci), 2018, 39(5): 669-674.

[8] Huang Z, Xia Y, Hu K, et al. Histone deacetylase 6 promotes growth of glioblastoma through the MKK7/JNK/c-Jun signaling pathway[J]. J Neurochem, 2020, 152(2): 221-234.

[9] Fuchs Y, Steller H. Programmed cell death in animal development and disease[J]. Cell, 2011, 147(4): 742-758.

[10] Moujalled D, Strasser A, Liddell JR. Molecular mechanisms of cell death in neurological diseases[J]. Cell Death Differ, 2021, 28(7): 2029-2044.

[11] Grad LI, Rouleau GA, Ravits J, et al. Clinical spectrum of amyotrophic lateral sclerosis (ALS)[J]. Cold Spring Harb Perspect Med, 2017, 7(8): a024117.

[12] Johnson EB, Gregory S. Huntington's disease: brain imaging in Huntington's disease[J]. Prog Mol Biol Transl Sci, 2019, 165: 321-369.

[13] Wirths O, Zampar S. Neuron loss in Alzheimer's disease: translation in transgenic mouse models[J]. Int J Mol Sci, 2020, 21(21): 8144.

[14] Canman CE, Lim DS. The role of ATM in DNA damage responses and cancer[J]. Oncogene, 1998, 17(25): 3301-3308.

[15] Ueno S, Sudo T, Hirasawa A. ATM: Functions of ATM kinase and its relevance to hereditary tumors[J]. Int J Mol Sci, 2022, 23(1): 523.

[16] Lee JH, Paull TT. Cellular functions of the protein kinase ATM and their relevance to human disease[J]. Nat Rev Mol Cell Biol, 2021, 22(12): 796-814.

[17] Salvador JM, Brown-Clay JD, Fornace AJ, et al. Gadd45 in stress signaling, cell cycle control, and apoptosis[J]. Adv Exp Med Biol, 2013, 793: 1-19.

[18] Sarkisian MR, Siebzehnrubl D. Abnormal levels of Gadd45alpha in developing neocortex impair neurite outgrowth[J]. PLoS One, 2012, 7(9): e44207.

[19] Nakanishi A, Minami A, Kitagishi Y, et al. BRCA1 and p53 tumor suppressor molecules in Alzheimer's disease[J]. Int J Mol Sci, 2015, 16(2): 2879-2892.

[20] Zhan Q. Gadd45a, a p53- and BRCA1-regulated stress protein, in cellular response to DNA damage[J]. Mutat Res, 2005, 569(1-2): 133-143.

[21] Putcha GV, Moulder KL, Golden JP, et al. Induction of BIM, a proapoptotic BH3-only BCL-2 family member, is critical for neuronal apoptosis[J]. Neuron, 2001, 29(3): 615-628.

[22] Puthalakath H, Huang DC, O'Reilly LA, et al. The proapoptotic activity of the Bcl-2 family member Bim is regulated by interaction with the dynein motor complex[J]. Mol Cell, 1999, 3(3): 287-296.

[23] 吴秀丽，徐琴，胡爽，等. 枸杞多糖对糖尿病周围神经病变大鼠PERK-CHOP通路及Bax、Bcl-2表达的影响[J]. 遵义医科大学学报，2023，46(5)：459-465.
Wu XL, Xu Q, Hu S, et al. Effects of Lyciumbarbarum polysaccharides on PERK-CHOP pathway, Bax and Bcl-2 expression in diabetic peripheral neuropathy rats[J]. J Zunyi Med Univ, 2023, 46(5): 459-465.

[24] Tong T, Ji J, Jin S, et al. Gadd45a expression induces Bim dissociation from the cytoskeleton and translocation to mitochondria[J]. Mol Cell Biol, 2005, 25(11): 4488-4500.

（编辑　余　菁）